NUMERICAL ANALYSIS OF COMPRESSOR BLADE FLUTTER IN MODERN GAS TURBINE ENGINES

Vasily Vedeneev[*], *Mikhail Kolotnikov*[**], *Pavel Makarov*[**]

[*] Faculty of mechanics and mathematics, Lomonosov Moscow State University, Russia
[**] Gas-turbine Engineering Research and Production Center "Salut", Russia

ABSTRACT

Blade flutter of the modern gas turbine engines is turning into one of the main issues that engine designers have to face. Today there is no general method for a reliable prediction of compressor blade flutter and flutter suppression in a wide range of engine operating regimes, especially at the engine design phase. Engine designers use internal criteria of their companies and approaches based on their own experience in engine design and refinement. In this paper we describe development of numerical method and present results of flutter onset prediction based on energy method. Analysis is limited by the condition of unstalled air flow through the blade passage, which is typical for compressor operating regimes. The problem is solved in the 3-D formulation.

The developed method is applied to flutter prediction of real compressor blade wheels of a modern gas turbine engine; results are verified by compressor and full engine test data. It is shown that the prediction of flutter onset is rather reliable. Influence of numerical parameters and modeling features on flutter prediction is studied.

NOMENCLATURE

f natural frequency
m number of nodal diameters
n rotor speed
$\bar{n}$ corrected rotor speed
N number of blades
W work done by the unsteady pressure during one period of blade oscillation
α $=2\pi m/N$, phase shift between the oscillations of neighbouring blades
ω $=2\pi f$, circular frequency

INTRODUCTION

Aircraft gas turbine engine designers were faced with compressor blade flutter in the middle of 50s while developing the second generation of jet engines. At the present day a huge theoretical and practical experience has been accumulated. Typically, regions of the various flutter types are plotted on the compressor operating map. They were developed by different researchers and are very similar (Shrinivasan, 1997, Bendiksen, 1988, Petrie-Repar et al., 2006, Marshall and Imregun, 1996, Bölcs and Suter, 1986). The scheme in Fig. 1 proposed by Bendiksen (1988) can be considered as an example. This map clearly shows that possible flutter regions are mainly located near surge line or significantly lower than the compressor operating line. When operating in these regions, the air flow in blade passages is unsteady with a lot of vortexes and shocks. The only exceptions are regions bounded by lines 3, 4, and 6. They lead to the blade flutter near operating line for unstalled flow. Recently Khorikov and Danilkin (2011) showed that region bounded by line 2 can also be located near the operating line.

The problem of numerical flutter prediction for compressor or fan blade wheels is associated with coupled aeroelastic problem, which first needs a solution for steady-state flow in blade passages. Modern computational codes, such as *ANSYS CFX, Star-CCM, Fluent, FlowVision*, etc.

provide reliable air flow parameters in blade passages near the operating line, where the flow is unstalled. For surge line (region 1) and for stalled flow (regions 5, 7) it is very difficult (and usually impossible) to determine reliable air flow parameters numerically, therefore numerical prediction of blade flutter boundaries for these regions usually cannot give any valid results. However, for the design phase of modern gas turbine engine compressors and fans the most important is to suppress flutter around the operating line with required safety margins, because this provides the ability for test validation of main characteristics of new compressors. Dynamic stress state of compressor or fan blades operating near surge line and in regions of stalled flow is typically determined experimentally during refinement of the engine.

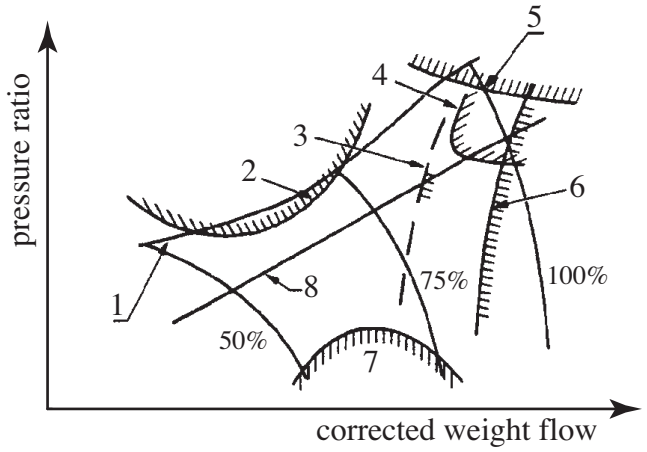

Fig. 1. Compressor operating map by Bendiksen (1988): 1- surge line; 2-subsonic stalled flutter; 3-bending-torsional flutter line (expected); 4- supersonic unstalled flutter induced by shocks; 5-supersonic stalled flutter; 6- supersonic unstalled flutter; 7 – choking flutter; 8-operating line

Basically, there are four methods for flutter prediction (Marshall and Imregun, 1996; Shrinivasan, 1997).

First ("direct") method is based on the direct numerical simulation of coupled blade-flow system. This method not only provides flutter regimes, but also gives limit cycle amplitude if flutter occurs. However, numerical difficulties of this approach, and necessity of great amount of the computational resources and time are main limitations of wide applications of this method. Besides, it is not easy to understand the physical nature of vibration amplification or damping.

The second ("frequency") method is based on calculation of eigenfrequencies of coupled fluid-structure system. Generally, eigenfrequencies of such system are complex because the system is not conservative. Positive imaginary part of the eigenfrequency is a criterion for flutter occurrence. This method is rather common and can be applied to flutter prediction of any aeroelastic structure. However, there are mathematical issues with finding eigenvalues of complex non-symmetric matrices; also computational resources comparable with the first method are necessary.

The third ("energy") method is based on calculation of the work done by the gas forces on displacements of elastic blade oscillating in natural mode over one cycle of oscillation. This method provides acceptable results if the natural mode shapes in vacuum and in flow are similar, which is almost always true, except for hollow blades. If the work is positive and greater than the work of damping forces, then flutter occurs. Advantage of this approach is that the analysis is relatively quick: for elastic blades only modal analysis should be conducted, whereas calculation of the work is a purely aerodynamic problem. The problem is uncoupled, and time savings are significant.

The fourth method of flutter prediction is the most used by gas-turbine engineers and is based on results of analysis and synthesis of practical experience of flutter occurrence in compressor and fan blades of real gas turbine engines after their refinement and in service. To formulate a criterion of flutter initiation both deterministic and probabilistic methods are used. Described criteria are

mainly one- or two-parametrical, though there are criteria with many more parameters (Lokshtanov et al., 1980). For each type of flutter the system of parameters is supplemented with limit values, established from study and generalization of flutter onset conditions in compressors-prototypes. These limits bound a possible flutter zone. One of the simplest criteria is the Strouhal number $Sh=\omega b/V$, where b is the blade chord of peripheral cross-section; ω is the circular blade frequency; V is the flow speed. Shrinivasan (1997) reported that for guaranteed flutter suppression in bending mode Sh must be greater than 0.8, for torsional mode it must be greater than 1.4. Wide application of this method by gas-turbine engine designers is reasonable, because it provides ability to use huge experience which has been accumulated from engine prototypes. Though these criteria should be used very carefully by compressor and fan designers from other companies as they could give unrealistic prediction for different compressor designs and operating parameters.

Based on analysis of solution methods shortly described above, we decided to use the third (energy) method for flutter analysis. Applications of this method in the 3-D formulation are presented below.

1. METHOD OF FLUTTER PREDICTION

We assume that the influence of the flow on natural blade modes and frequencies is negligible. This assumption is valid for the case of sufficiently stiff blades, when flow disturbances excited by small blade vibration have no significant action on blade eigenmodes. Therefore, the air flow can result only in small additional damping (for stability case), or additional energy inflow (for flutter case) without change of natural modes and frequencies. Kinetic energy equation for blade in coordinate system rotating with the wheel is

$$\frac{dE(t)}{dt} = A(t), \tag{1}$$

where $E(t)$ is the kinetic energy, $A(t)$ is the power of internal and external forces. Neglecting structural damping and viscous forces of the flow, we assume that the only force is the pressure distributed along the blade surface. Then change of kinetic energy over the cycle of oscillation is:

$$\Delta E = W = \int_{t_0}^{t_0+T}\iint_S p(x,y,z,t)\cdot\vec{n}(x,y,z,t)\cdot\vec{\upsilon}(x,y,z,t)dsdt, \tag{2}$$

where $T=1/f$ is the blade oscillation period (f is the natural frequency), S is the blade surface, p is the flow pressure, n is the blade surface normal, υ is velocity of the blade points.

While the flow influence on the blade oscillations is small, the work W done over actual (growing or damped) oscillation is also small. The work over harmonic (constant amplitude) oscillation is different from actual work by a second-order infinitesimal term, which is neglected. Harmonic oscillation shape is assumed to be obtained from modal analysis using standard engineering software.

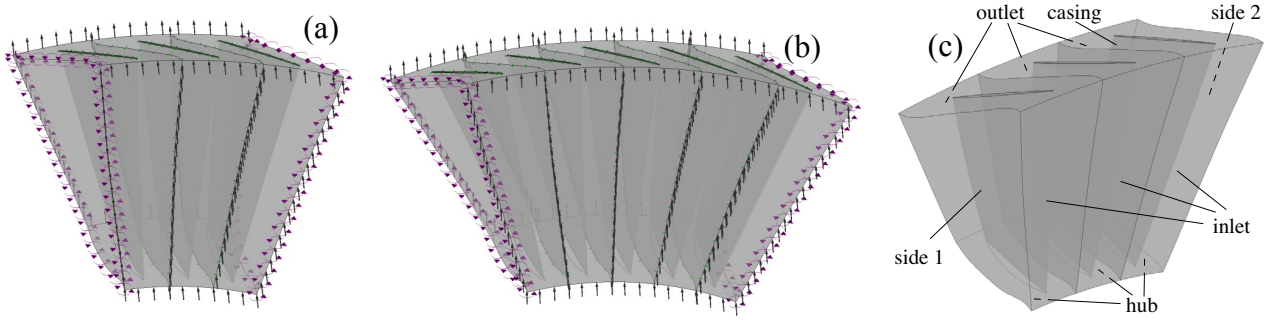

Fig. 2. Models of three (a) and five (b) consecutive blade passages. Boundary conditions (c).

Thus we calculate the work done by unsteady pressure over specified oscillations of the blade during one oscillation period. The following inequality is a criterion of flutter:

$$W > 0. \tag{3}$$

Finite-volume model of gas flow consists of three or five consecutive blade passages of a one stage (Fig. 2a, b). For unsteady fluid flow analysis initial and boundary conditions are extracted from steady-state analysis of the flow in the full compressor (where all stages are modeled), verified by full-scale compressor tests. Namely, we specify distribution of total pressure, total temperature, velocity, and turbulence parameters at the inlet (Fig. 2c), and distribution of static pressure at the outlet. No-slip condition is assigned at solid body surfaces: hub, blades, and casing; for the latter surface the boundary condition is applied in rotating coordinate system. Condition of rotational periodicity connects flow parameters at side 1 and side 2 (Fig. 2c).

Mesh displacement in form of wheel natural oscillations with specified number of nodal diameters is applied to each blade surface: $\vec{u}(x,y,z,t) = A \cdot \sin \omega t \cdot (L_n(x,z))$, where A and $\omega=2\pi f$ are blade oscillation amplitude and circular frequency, $L_n(x, z)$ is a function describing the mode shape. We use 10^{th}-order Lagrange interpolation polynomial for interpolating FEM mode shape results and transferring them to the CFD code.

For modeling forward (or backward) traveling wave, which is typical for cascade flutter (Kolotnikov et al., 2008), phase lag $sin(\omega t-\alpha)$ and lead $sin(\omega t+\alpha)$ with respect to the middle blade are specified for neighboring blades, where the phase shift $\alpha=2\pi m/N$ corresponds to the number of nodal diameters m. In case of five-blade model the phase shift for the side blades is $\pm 2\alpha$.

Let us prove that with these assumptions the work done by steady component of pressure during one harmonic oscillation is zero. Indeed, Kielb et al. (2006) showed that the work associated with the steady pressure can be non-zero if there is a phase shift between different blade points (i.e., eigenmodes are complex). However, we assume that each blade oscillates in form of standing wave, such that there is no phase shift between points of each blade (though the phase shift between different blades is non-zero), hence the eigenmodes are real. In this case the work done by the steady pressure is zero. Therefore we will assume that the pressure p in (2) is the unsteady pressure due to blade oscillation.

In accordance with the procedure described, flutter analysis consists of four stages:

1. Modal analysis of elastic blades. Interpolation of mode shapes by Lagrange polynomials.
2. Steady-state flow analysis in compressor.
3. Unsteady flow analysis of a certain compressor stage with blades oscillating (i.e. fluid mesh moving) in specified mode obtained at step 1.
4. Calculation of work (2) done by pressure for the middle blade and check of criterion (3).

Steps 3 and 4 are executed for each natural mode potentially sensitive to flutter. Work is calculated for the last of several simulated cycles of oscillations, such that the flow response to the blade oscillations is pure harmonic. Calculations show that three periods is typically enough to have harmonic response (see section 2.4)

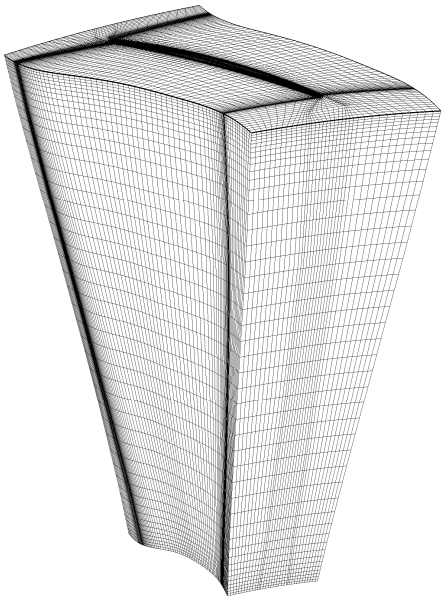

Fig. 3. “Basic” mesh (~200000 control volumes per passage).

Structural modal analysis is performed using *Ansys Mechanical* FE software. For fluid flow analysis we use *Ansys CFX*, version 12.1. Note that we checked that newer version 13.0 gives the same results as 12.1, whereas older version 11.0 is unworkable. This is due to incorrect calculation of the pressure term when solving Navier-Stokes equations with deformning mesh; this bug was fixed in version 12.1. Reynolds-averaged Navier-Stokes equations with k-ε turbulence model are solved. For polynomial interpolation and calculation of work done by unsteady pressure a special software has been developed.

Flutter onset predictions presented in this paper are obtained for two fan wheel models (Table 1). Each wheel is analyzed in two modifications:

- Wheel 1 with shrouded and with cantilever blades. Fixed rotation speed specific for the throttle regime (compressor operating near region 3 in Fig. 1) is studied. Air flow parameters correspond to zero altitude and zero Mach number at the engine inlet.
- Wheel 2 with shrouded blades. Rotor corrected speeds of 77 and 100% are analyzed.

When investigated wheel 1 we studied numerical convergence and implementation features (number of blades in the model, oscillation amplitude, etc); results are compared with test data. When analyzed wheel 2 we studied effects of physical parameters, such as blade mode shape, assembling interference between contact surfaces of mid-span shroud, blade tip clearance, inlet flow incidence angle, and others.

Table 1. Parameters of the wheels considered (index "0.5" means the middle of the blade span)

		Wheel 1	Wheel 2	
Number of blades	N	45	37	
Rotor speed	n, Hz	136.0	159.5 ($\overline{n}$ = 77%)	170.0 ($\overline{n}$ = 100%)
Inner to outer diameter ratio	$= d/D$	0.570	0.435	
Relative blade spacing	$= t_{0.5}/b_{0.5}$	0.800	0.766	
Blade aspect ratio	$= h/b_{0.5}$	3.120	3.554	
Mid-span shroud location	$= h_s/h$	0.710	—	0.772

2. ANALYSIS OF CONVERGENCE AND NUMERICAL EFFECTS

Three-blade model of wheel 1 was used for analysis of convergence and effect of numerical parameters. We calculated the work done by unsteady pressure over a cycle of oscillations in mode 1 for m=0 (all blades oscillate with the same phase).

The following parameters were selected as "basic" for the analysis. Single precision was used (all variables are of *float* type). Time step was selected such that there are 100 steps per one cycle of oscillation. Three periods were analyzed; work was calculated for the last period (i.e. for steps 200…300). Root mean square convergence residual for equations was set to be $5 \cdot 10^{-5}$ for each time step (maximum residual turns out to be $\sim 10^{-3}$). Number of spatial iterations at each time step was higher than 10 and less than 100. Mesh consisted of approximately 200 000 control volumes (Fig. 3). Work calculated for the first natural mode is denoted by "1" in Fig. 4. During convergence study we calculated the same work with one of the parameters taken with higher precision. At each run overall convergence criteria, such integral conservation laws, were checked.

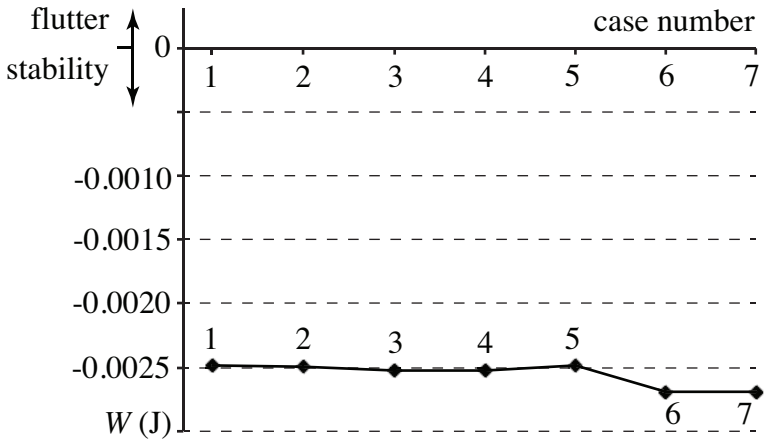

Fig. 4. Influence of numerical effects on the work done by unsteady aerodynamic pressure.

2.1. Precision of unsteady aerodynamic problem solution. Calculations were conducted with double precision (all variables were of *double* type). Result is denoted by "2" in Fig. 4.

2.2. Convergence in time step. Calculation with 4-times reduced time step was conducted. One period included 400 iterations, total simulation time (3 periods) consisted of 1200 steps. Result is denoted by "3" in Fig. 4.

2.3. Convergence in residuals. This was checked together with time step reduction.

Result shown in Fig. 4, point "4", was obtained at a two times smaller time step (600 iterations for the full runtime) and maximal residual of 10^{-4} (RMS residual of ~10^{-6}).

2.4. Number of oscillation periods. To check sufficiency of 3 periods for harmonicity of the flow at the last period, additional analysis was conducted with 3 more periods simulated. Work was calculated at the 6th period, result is denoted by "5" in Fig. 4.

2.5. Convergence in mesh. Calculations were conducted using refined meshes, of 430 000 and 800 000 control volumes per each blade passage. Results are shown in Fig. 4 as "6" and "7.

It is seen in Fig.4 that the work done by pressure during the last oscillation period is changed insignificantly in all cases, except a slight change due to mesh refinement; it proves sufficiency of accepted basic parameters. In order to investigate actual mesh influence in more detail, we analysed the whole range of nodal diameters for the first two modes. Results shown in Fig. 5 prove that convergence in mesh is achieved at the mesh size of 200 000 control volumes per passage.

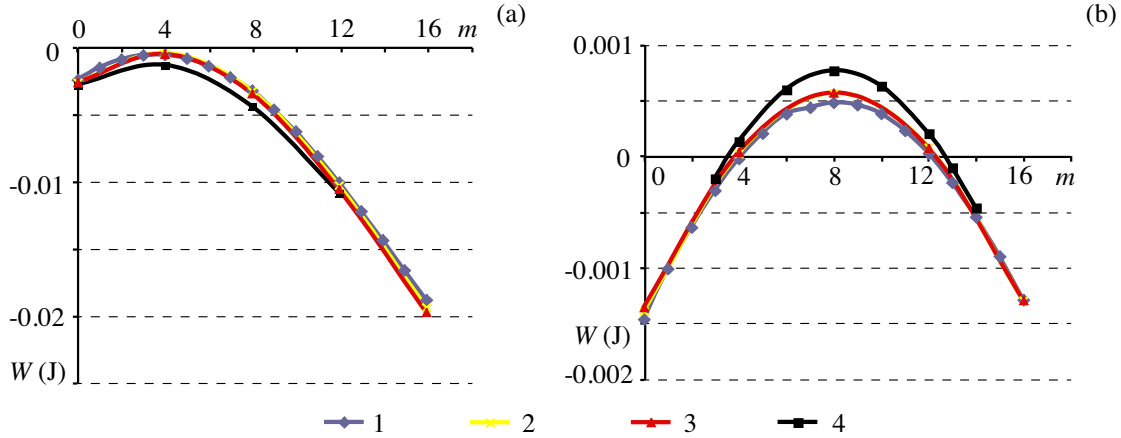

Fig. 5. Work vs *m*. Mode 1 (a), 2 (b). Curves 1-3: 3-blade model, mesh size is 200, 430, 800 thousands of volumes per blade passage. Curve 4: 5-blade model, mesh size is 200 000 volumes.

Analysis of 3-blade model of wheel 2 showed insignificance of the following parameters: oscillation amplitude, inlet turbulence level, deviation of the flow incidence angle. However, tension in mid-span shroud and deviation of mode shape essentially change flutter boundary. Modeling of mid-span shroud in aerodynamic analysis will be studied in section 3.2. Also, number of blades in the model (5 vs 3-blade) was studied (Fig. 5, curve 4) and appeared to be insignificant for the work. This means that only blades neighboring to the middle blade affect flutter. Thus, using of 3-blade model is enough for reliable flutter prediction. This fact was also obtained in investigation of aerodynamic influence coefficients in plate cascades (Samoylovich, 1969).

"Basic" parameters were used in studies described below. We used 3-blade models and forward ($m>0$) or beckward ($m<0$) traveling deformation wave with fixed number of nodal diameters.

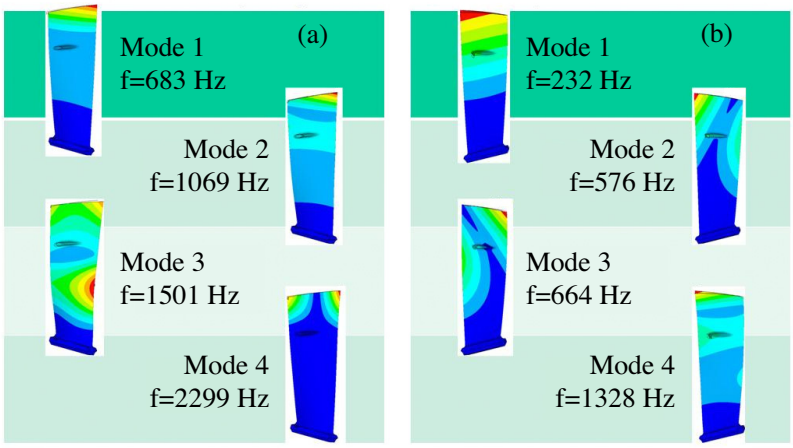

Fig. 6. First natural modes of the wheel 1: (a) shrouded, (b) cantilever. Colors represent displacement amplitude.

3. RESULTS OF NUMERICAL FLUTTER PREDICTION IN BLADE WHEELS

3.1. Wheel 1.

Calculation of work done by pressure for first four natural modes was conducted. Each mode was analyzed in a full range of possible numbers of nodal diameters. Oscillations are specified in form of forward (along the wheel rotation) or backward traveling wave. Amplitude was such that maximum blade stress was 5×10^7 Pa. The first four frequencies and mode shapes are shown in Fig. 6 for the wheel 1 with and without mid-span shroud.

Work done over modes of cantilever blades is shown in Fig. 7. Work of the 1st and 4th modes is negative, while for the 2nd and 3rd modes it is positive for 5…11 and 5...16 nodal diameters, respectively. Therefore, for this wheel we predict blade flutter in the 2nd and 3rd modes.

Work calculated for the same wheel with shrouded blades is shown in Fig. 8. For the first four natural modes the work is negative. We therefore predict stability of this blade wheel.

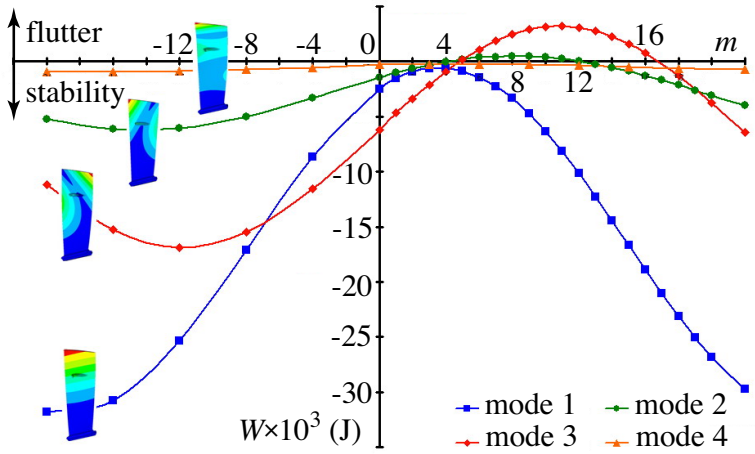

Fig. 7. Work done by unsteady pressure vs. number of nodal diameters for the wheel 1 with cantilever blades.

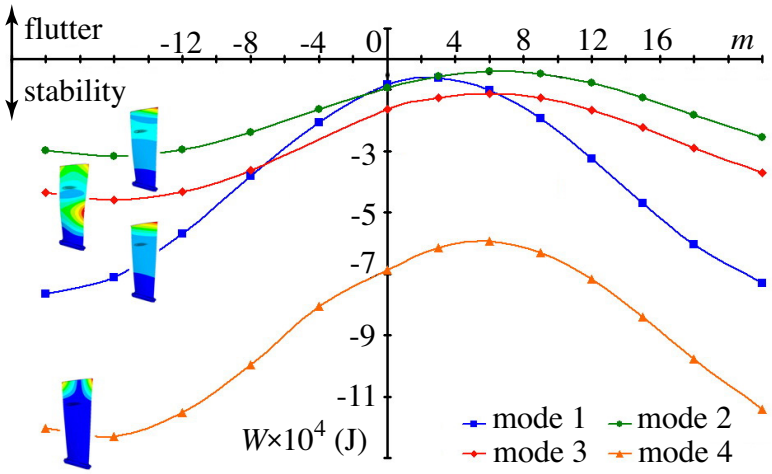

Fig. 8. Work done by unsteady pressure vs. number of nodal diameters for the wheel 1 with shrouded blades.

3.2. Wheel 2.

For the first and second natural modes of the shrouded wheel 2, flutter analysis has been conducted for two operating regimes: $\overline{n} = 77\%$ and $\overline{n} = 100\%$. First, we studied influence of tension in mid-span shroud on flutter prediction and it turned out to be extremely important due to significant change of the mode shapes (Fig. 9a, b). In Fig. 9 natural modes of untensioned blade wheel were calculated for each number of nodal diameters *m*. On the contrary, modes of tensioned wheel with different number of nodal diameters were modeled by specifying only phase shift between neighboring blades, while blade mode shape was unchanged. This simplified approach was used due to complexity of mode shapes of tensioned shrouded wheel: eigenmodes cannot be grouped by mode type (bending, torsional, etc), nodal diameters, or frequency band; each mode looks like a mixture of different untensioned blade modes, they cover a wide range of frequencies.

Work done by unsteady pressure over the first two natural modes of tensioned wheel is shown in Fig. 10 by continuous curves. It is seen that both modes are damped at $\overline{n} = 100\%$, while at $\overline{n} = 77\%$ the second mode (*f*=910 Hz) with 5…9 nodal diameters is in flutter zone.

Influence of mid-span shroud modeling in aerodynamic analysis was studied at $\bar{n} = 77\%$ regime (note that the shroud was always modeled in modal analysis). Results are present in Fig. 10 by dashed curves. It is seen that neglecting mid-span shroud in unsteady flow analysis increases the work for both modes for any number of nodal diameters. In other words, neglecting the shroud is conservative.

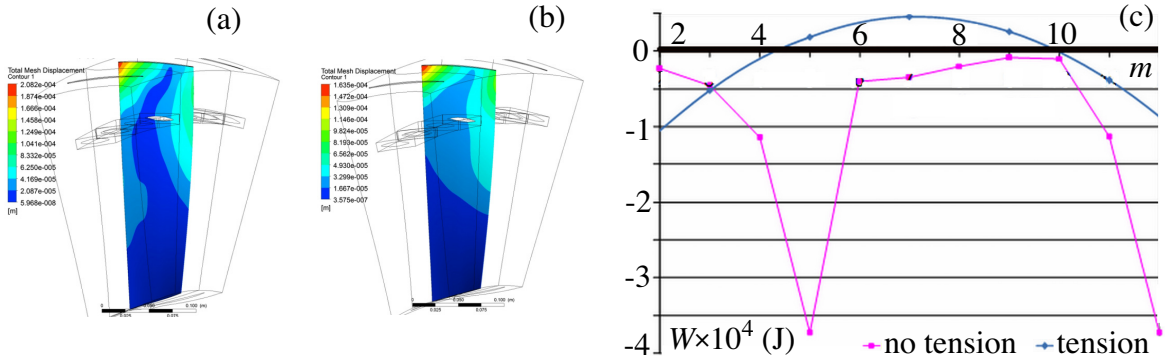

Fig. 9. Effect of tension in mid-span shroud of the wheel 2 on the 2nd natural mode at $\bar{n}$ =77%: (a) untensioned blades (m=9); (b) tensioned blades; (c) work done by unsteady pressure vs. m.

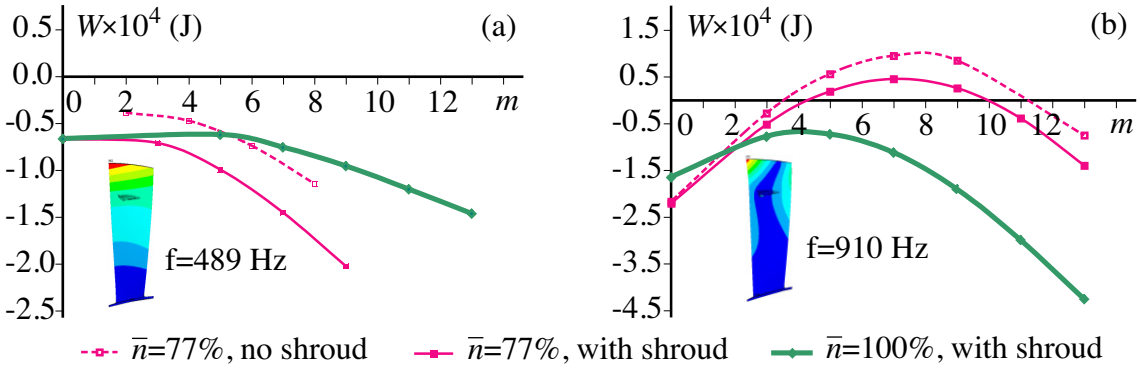

Fig. 10. Work done by unsteady pressure vs. number of nodal diameters for the wheel 2; effect of shroud modeling in aerodynamic analysis: (a) 1st (bending) mode, (b) 2nd (bending-torsional) mode.

4. EXPERIMENTAL VALIDATION OF NUMERICAL RESULTS

Validation of numerical flutter prediction for the wheels 1 and 2 was conducted at special full-scale tests of the gas turbine engine.

4.1. Test facility, strain gauge locations and test procedure

Experimental detection of compressor wheel flutter was conducted using special test facility (Fig. 11) with simulation of altitude, speed and environmental air conditions, including required flow irregularity, flow pressure and temperature at the engine inlet.

Air flow at the inlet of the fan has average values of total pressure and stagnation temperature equal to averaged values of parameters of the fan operating at flight conditions on an aircraft with required margins of safety. From compressor station the air flows through refrigerating units or air heaters providing required pressure and temperature values.

Blades of wheels 1 and 2 were prepared with strain gauges located in regions of maximum stress for the first four modes, which are usually most unstable (Fig. 12). Maximum stress zones for these modes were obtained by a numerical study and during laboratory tests on vibration-testing machine. In order to perform phase shift analysis for detection of number of nodal diameters in coupled blade-disc-flow vibrations, several consecutive blades were prepared with strain gauges.

Multi-channel high-efficiency recording apparatus was used to record and control data from strain gauges. It provides required discretization frequency of signal processing with spectral

resolution of 1 Hz and amplitude accuracy of 2%. Connection between strain gauges and processing apparatus is established through multi-channel remote converter.

Processing of data from strain gauges consisted of analysis of spectral structure and interconnection of data from consecutive blades using narrow-band spectral analysis.

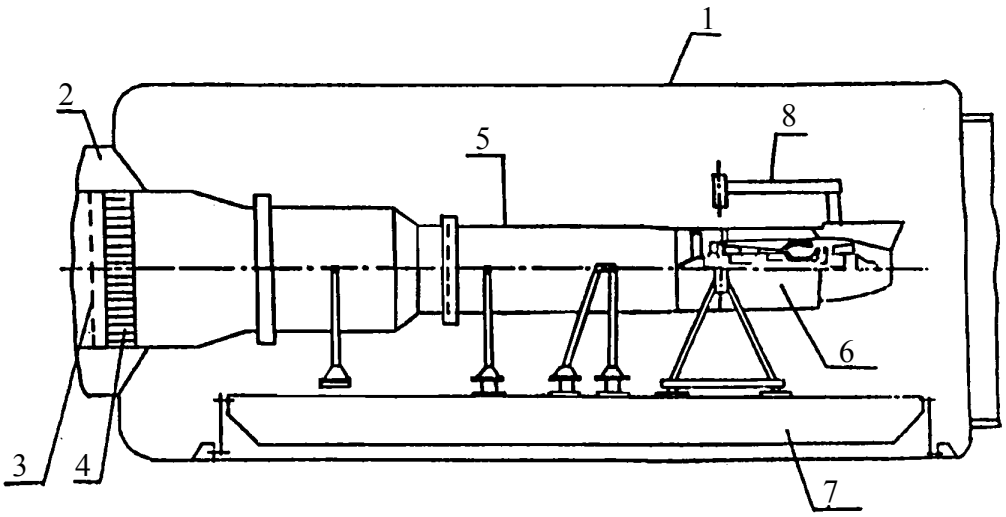

Fig. 11. Sketch of the test facility for blade flutter detection during engine test: 1 – pressure chamber; 2 – receiver; 3 – honeycomb; 4 – velocity strainer; 5 – attached piping; 6 – engine; 7 – dynamometering platform; 8 – motor frame.

4.2. Test results

Two modifications of the wheel 1 were tested: blades with mid-span shroud and cantilever blades. Analysis of strain gauge data from the shrouded wheel shows no flutter in the whole range of the fan speed. In the range of n=40-60%, i.e. of relatively low rotation speeds, where the flow is unstable, random forced vibrations with low amplitudes were detected. At n=80% resonant vibrations occurred in the first four modes with acceptable level of stress amplitudes (Fig. 13).

Signal processing from strain gauges of the wheel 1 with cantilever blades shows that starting from rotor speed n=55% non-resonant vibrations occur in modes 2, 3, 4 with high total level of vibration stress (Fig. 14a). Relative spectral analysis both from neighboring and remote blades shows flutter onset in 2nd (m=6…7) and 3rd (m=5…14) natural modes (Fig. 14b). Oscillations in the 4th mode were classified as random forced vibrations.

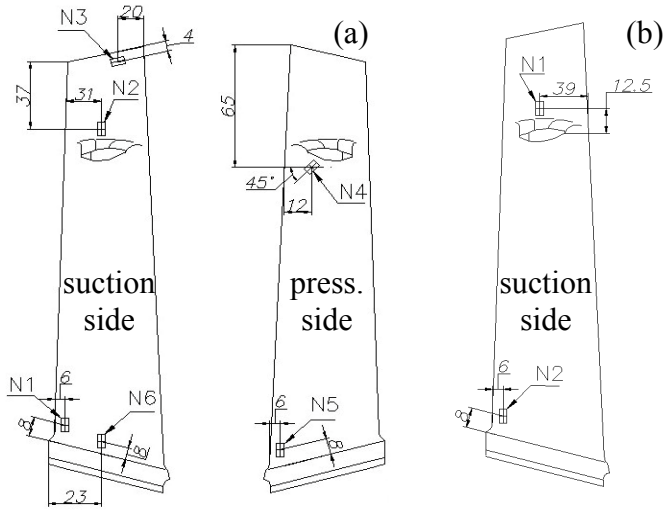

Fig.12. Strain gauge locations on tested blades: (a) wheel 1; (b) wheel 2.

Thus test results of the wheel 1 are in a full agreement with numerical predictions (section 3.1). Indeed, predicted stability and flutter regimes coincide with test stability and flutter regimes, moreover, flutter was observed in the same modes and nodal diameters that were predicted to be unstable (compare Figs. 7 and 14b).

Results of signal processing from strain gauges of the shrouded blade wheel 2 showed that there is no flutter at $\overline{n} = 100\%$. However, at $\overline{n} = 77\%$ flutter vibrations occurred in the 2nd mode with forward-travelling wave and number of nodal diameters m=6...8 (Fig. 15). These results demonstrate excellent agreement between test data and numerical prediction of flutter onset (Fig. 10b) for the considered fan wheel.

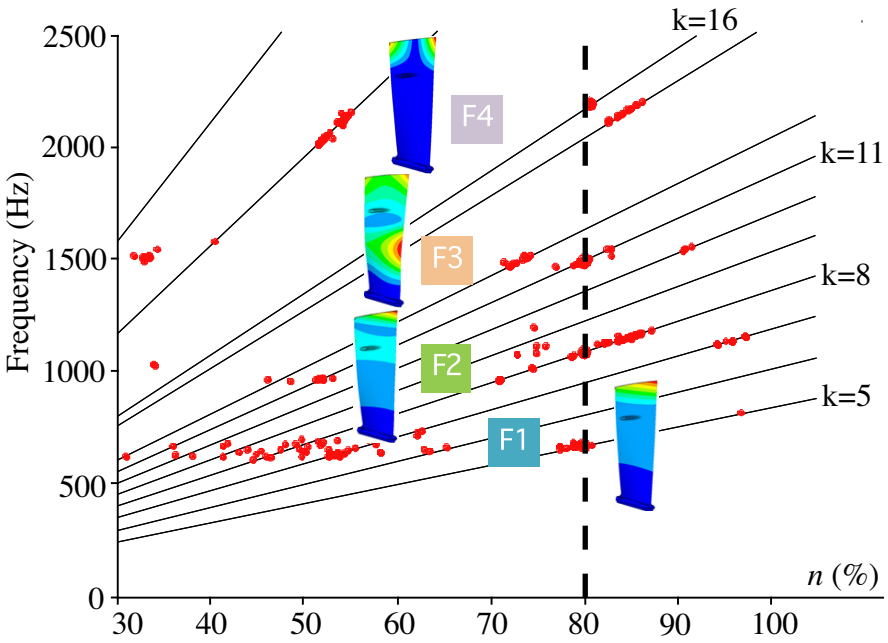

Fig.13. Strains measured for shrouded blade wheel 1 (Campbell diagram). Red dots represent spectral peaks with amplitudes exceeding noise level.

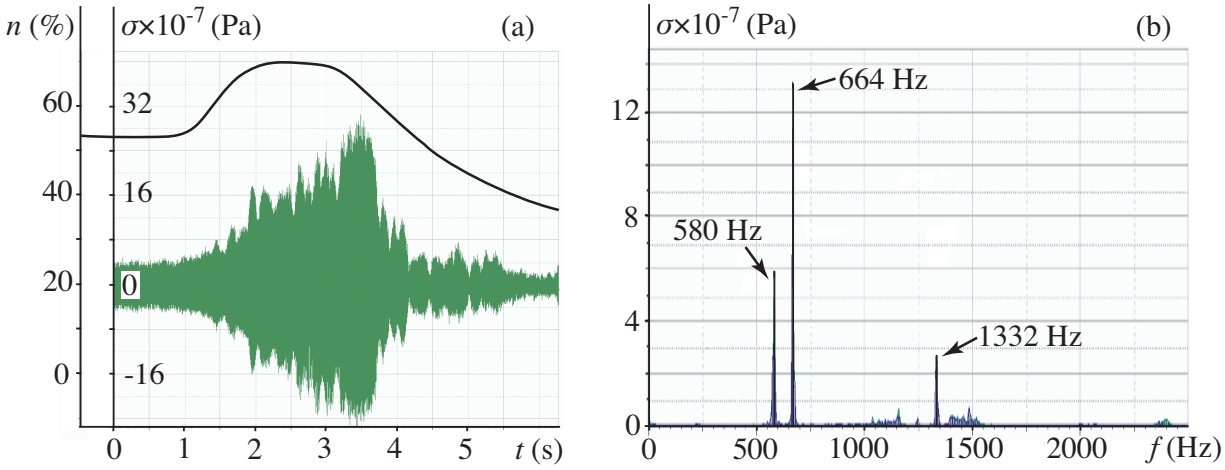

Fig.14. Test results of the cantilever blade wheel 1: (a) rotation speed and blade stress; (b) spectrum of the blade stress during flutter.

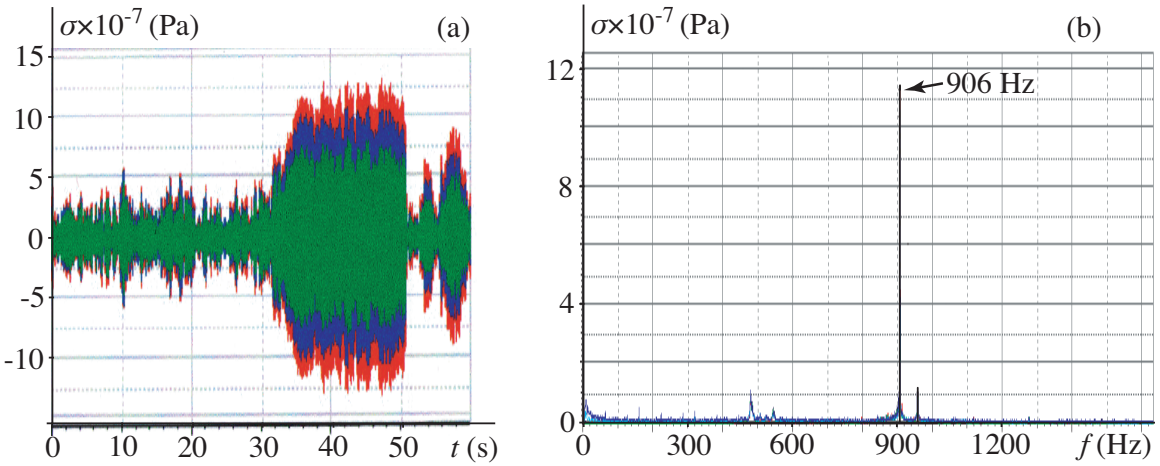

Fig.15. Test results of the wheel 2 at $\bar{n} = 77\%$: (a) blade stress (colors represent data from different strain gauges); (b) spectrum of the blade stress during flutter.

CONCLUSIONS

Flutter prediction procedure based on energy method is developed. It is valid for the unstalled flow conditions, which are typical for operating regimes. Two examples of application of this procedure to real blade wheels are given. Both are verified by full-scale tests in two operating regimes: stable and fluttering.

The influence of numerical parameters, as well as blade design parameters and assembling conditions on flutter onset is studied. It is shown that there is no significant influence of increased numerical accuracy, flow angle of attack variation within manufacturing tolerance, inlet level of turbulence, and blade oscillation amplitude. Tension in mid-span shroud has considerable influence on flutter prediction, although inclusion of mid-span shroud in the aerodynamic model does not affect much. It is shown that for reliable flutter prediction it is enough to use 3-blade one-stage aerodynamic model and to calculate work done by unsteady pressure for the middle blade during the third oscillation period.

The procedure developed can be used in the design of new compressors that have non-typical blade or disc shape for prediction of flutter onset. It is also suitable for blade wheel design or re-design for flutter suppression near compressor operating regimes with unstalled air flow.

ACKNOWLEDGEMENTS

The work is partially supported by grant of Russian Foundation for Basic Research 11-01-00034 and grant NSh-1303.2012.1.

REFERENCES

1. Shrinivasan A.V. Flutter and Resonant Vibration Characteristics of Engine Blades. Journal of Engineering for Gas Turbines and Power. Vol. 119, No. 3, 1997, pp. 742-775.

2. Bendiksen O. Recent Developments in Flutter Suppression Techniques for Turbomachinery Rotors. Journal of Propulsion and Power. Vol. 4, No. 2, 1988, pp. 164-172.

3. Petrie-Repar P., McGhee A., Jacobs P., Gollan R. Analytical Maps of Aerodynamic Damping as a Function of Operating Condition for a Compressor Profile. Proceedings of ASME Turbo Expo 2006. May 8-11, Barselona, Spain.

4. Marshall J.G., Imregun M. A Review of Aeroelasticity Methods with Emphasis on Turbomachinery Applications. Journal of Fluids and Structures. Vol. 10, No. 3, 1996, pp. 237-267.

5. Bölcs A., Suter P. Transsonische Turbomaschinen. Wissenschaft und Technik. Taschenausgabe, Karlsruhe, G. Braun, 1986.

6. Khorikov A. A., Danilkin S. Y. Research of the fan blades flutter on the stalling airflow mode. Herald of Samara State Aerospace University. Vol. 2, No. 3 (27), 2011, pp. 57-63.

7. Lokshtanov E.A., Mikhailov V.M., Khorikov A.A. Probabilistic flutter prediction of turbomachine blades. Aeroelasticity of turbomachine blades. Kiev: Naukova dumka, 1980, pp. 73-81.

8. Kolotnikov M. E., Makarov P. V., Sachin V. M. Study of wide-chord blade dynamic strength during tests. Aviation and space techniques and technology. No. 9 (56), 2008, pp.58-64.

9. Kielb R., Barter J., Chernysheva O., Fransson T. Flutter design of low pressure turbine blades with cyclic symmetry modes. Unsteady aerodynamics, aeroacoustics and aeroelasticity of tubomachines. Springer, 2006, pp. 41-52.

10. Samoylovich, G.S. Unsteady Flow and Aeroelastic Vibrations in Turbomachine Cascades. Moscow: Nauka, 1969.